



Published in final edited form as:

Cancer Discov. 2015 February ; 5(2): 135–142. doi:10.1158/2159-8290.CD-14-1156.

Biallelic Mutations in *BRCA1* Cause a New Fanconi Anemia Subtype

Sarah L. Sawyer^{1,*}, Lei Tian^{2,*}, Marketta Kähkönen³, Jeremy Schwartzentruber⁴, Martin Kircher⁵, University of Washington Centre for Mendelian Genomics, FORGE Canada Consortium, Jacek Majewski^{6,7}, David A. Dymant¹, A. Micheil Innes⁸, Kym M. Boycott¹, Lisa A. Moreau⁹, Jukka S. Moilanen¹⁰, and Roger A. Greenberg²

¹Children's Hospital of Eastern Ontario Research Institute, University of Ottawa, Ottawa, ON, Canada ²Departments of Cancer Biology and Pathology, Abramson Family Cancer Research Institute, Basser Research Center for BRCA, Perelman School of Medicine, University of Pennsylvania, 421 Curie Blvd, Philadelphia, PA 19104-6160 ³Pirkanmaa Hospital District, Fimlab Laboratories, Laboratory of Clinical Genetics, Tampere, Finland ⁴Wellcome Trust Sanger Institute, Hinxton, Cambs, United Kingdom ⁵Department of Genome Sciences, University of Washington, Seattle, WA, USA ⁶Department of Human Genetics, McGill University, Montréal, QC, Canada ⁷McGill University and Genome Quebec Innovation Centre, Montréal, QC, Canada ⁸Department of Medical Genetics and Alberta Children's Hospital Research Institute for Child and Maternal Health, University of Calgary, Calgary, Alberta, Canada ⁹Departments of Radiation Oncology and Pediatrics, Dana-Farber Cancer Institute, Harvard Medical School, Boston, MA ¹⁰Department of Clinical Genetics and Medical Research Center Oulu, Oulu University Hospital and University of Oulu, Oulu, Finland

Abstract

Deficiency in BRCA dependent DNA inter-strand crosslink (ICL) repair is intimately connected to breast cancer susceptibility and to the rare developmental syndrome, Fanconi Anemia (FA). *Bona fide* FA proteins, BRCA2 (FANCD1), PALB2 (FANCN), and BRIP1 (FANCI) interact with BRCA1 during ICL repair. However, lack of detailed phenotypic and cellular characterization of a patient with biallelic *BRCA1* mutations has precluded assignment of *BRCA1* as a definitive FA susceptibility gene. Here we report the presence of biallelic *BRCA1* mutations in a woman with multiple congenital anomalies consistent with a FA-like disorder and breast cancer at age 23. Patient cells exhibited deficiency in BRCA1 (FANCS) and Rad51 localization to DNA damage

CORRESPONDENCE: Roger A. Greenberg, Address: Department of Cancer Biology, Abramson Family Cancer Research Institute, University of Pennsylvania School of Medicine, 421 Curie Blvd, BRB II/III Rm 513, Philadelphia, PA 19104-6160, USA, Tel: 215-746-2738, rogergr@mail.med.upenn.edu.

*These authors contributed equally to this work

DISCLOSURE of POTENTIAL CONFLICTS of INTEREST

The authors declare no conflict of interests. The authors declare no competing financial interest.

AUTHOR CONTRIBUTIONS

This study was designed by K.M.B., S.L.S., J.S.M., L.T., and R.A.G. Pedigree analysis and clinical phenotype analysis was performed by J.S.M. with further review by D.A.D. and A.M.I. Whole exome sequencing and analysis by J.S., J.M., M.K (Martin Kircher). Analyses of variant files (only) were performed by S.L.S., D.A.D. and A.M.I. Chromosome fragility analysis on lymphocytes was performed by M.K (Marketta Kähkönen). and on fibroblasts by L.A.M. All other experimental analysis of patient cells was performed by L.T. with guidance from R.A.G. The manuscript was written by S.L.S., L.T., and R.A.G.

sites, combined with radial chromosome formation and hypersensitivity to ICL inducing agents. Restoration of these functions was achieved by ectopic introduction of a *BRCA1* transgene. These observations provide evidence in support of *BRCA1* as a new Fanconi anemia subtype (FA-S).

Keywords

BRCA1; DNA repair; Fanconi Anemia

INTRODUCTION

The identification of mutations within 16 different Fanconi Anemia (FA) genes has been particularly instructive regarding how specific aspects of DNA crosslink repair impact human disease phenotypes (1–4). ICL repair is initiated by a core FA protein complex, which requires monoubiquitination of the FANCD2 and FANCI proteins for localization to DNA crosslinks. ICL recognition by the canonical ubiquitinated D2-I complex is thought to direct subsequent DNA replication-dependent processing of ICLs in S-phase to DNA double-strand break (DSB) intermediates that require BRCA1 and BRCA2 for homology directed DNA repair (5, 6). Recent evidence also implicates the BRCA proteins and Rad51 at earlier stages of ICL repair (5, 7, 8). The putative multifactorial involvement of individual FA genes in different aspects of ICL repair may account for the diverse spectrum of phenotypes exhibited in this syndrome. Notably, biallelic carriers of BRCA2 (FANCD1) and PALB2 (FANCN) display a severe FA phenotype and solid tumor development (9–11), whereas this is not observed in patients with mutations in canonical FA genes.

Given the many connections between BRCA1 and both the D2-I and BRCA2-PALB2 arms of ICL repair (2, 3), it is somewhat paradoxical that biallelic *BRCA1* mutations have not been previously identified as a cause of FA. Despite high carrier frequencies in Ashkenazi Jewish populations, no patient with biallelic mutations in *BRCA1* had been reported until recently (12), presumably because most combinations of deleterious *BRCA1* mutations would result in embryonic lethality. This individual harbored a hypomorphic *BRCA1* BRCT (BRCA1 C-terminal) repeat missense allele in trans to a frameshift mutation within *BRCA1* exon 11. She presented with short stature, developmental delay, microcephaly, and ovarian cancer at age 28 with hypersensitivity to carboplatin based chemotherapy. Although this case report established that biallelic deleterious *BRCA1* mutations allow viability in humans, the absence of a cell line from this patient and the lack of extensive phenotypic examination precluded definitive assessment of whether biallelic *BRCA1* mutations cause FA. We report here on a second patient harboring biallelic *BRCA1* mutations, early onset breast cancer, and multiple developmental and cellular anomalies consistent with a new FA subtype.

RESULTS

The proband presented at birth with microsomia and dysmorphic features (Fig. 1A). Growth parameters were less than the 0.4 percentile at term (birth weight 1990g, height 40.5 cm, head circumference (HC) 27 cm), and subsequent catch-up growth was not evident at 25 years of age (weight 40 kg, –3.03 S.D.; 135 cm tall, –4.35 S.D.; HC 48.5 cm, approx. –4 to –5 S.D.). Additional congenital abnormalities included sparse hair, upslanted palpebral

fissures, blepharophimosis, a narrow palate, dental malocclusion, a high-pitched and hoarse voice, hyper and hypopigmented skin lesions, duodenal stenosis and a slightly enlarged left kidney. She has proximally inserted thumbs (Fig. 1A), 2nd digit camptodactyly, 2–3 toe syndactyly and hyperextensible knees as well as a history of hip dislocation. Conductive hearing loss was diagnosed at 4 years of age. Bone age at 2y 3m was delayed (1y and 6m (–2S.D.)), but had normalized by 9 years. The patient also has mild intellectual disability with significantly delayed speech. At 23 years of age she was diagnosed with ductal breast carcinoma that was estrogen and progesterone receptor positive and Her2 negative. Mastectomy was performed followed by treatment with docetaxel, fluorouracil-epirubicin-cyclophosphamide and radiation therapy. A prophylactic mastectomy was performed on the contralateral breast at age 25. The patient did not experience unusual treatment associated toxicity and has not been diagnosed with bone marrow failure to date.

To identify the molecular basis for her syndromic presentation, the patient was originally ascertained as part of an international effort to identify gene(s) for Dubowitz syndrome (OMIM 223370) through the FORGE (Finding of Rare Disease Genes) Canada consortium. Dubowitz syndrome is a disorder characterized by microcephaly, cognitive and growth delay and increased risk of malignancy and immunodeficiency, and is suspected to be genetically heterogeneous. Whole exome sequencing was performed on patient genomic DNA as part of this analysis. Sequencing results revealed biallelic compound heterozygous variants in the *BRCA1* gene. A 4 bp deletion at the beginning of exon 10 (NM_007294:c.594_597del) was found on one of the alleles, which predicts a truncated protein with N-terminal 198 amino acids of BRCA1 followed by an out of frame stretch of 35 amino acids within exon 11 not related to the canonical BRCA1 protein (p.Ser198Argfs*35). The second allele showed a point mutation in exon 18 (NM_007294: c.5095C>T), resulting in a single amino acid substitution (p.Arg1699Trp) within the BRCT repeats (Fig. 1B). This missense mutation has been previously reported as a pathogenic mutation, predisposing carriers to breast and ovarian cancer (13–15). There were no other compelling variants that explained her developmental phenotype, and none that were shared with other patients diagnosed with Dubowitz syndrome.

As *BRCA1* is a major gene related to hereditary breast cancer, we performed further pedigree and genetic analysis of the family (Figs. 1B and 2A). The proband is the second of three children born to non-consanguineous Finnish parents. Segregation analysis in the family did not identify any other siblings with biallelic mutations, or any with the syndromic features seen in the proband. Sibling III: 3 was found to be heterozygous at the c.C5095 position and has no history of cancer. The *BRCA1*:c.594_597del and c.5095C>T missense mutations were confirmed to be maternally and paternally derived, respectively, which is consistent with autosomal recessive inheritance. The proband's mother (II: 4) carries the *BRCA1*:c.594_597del and presented with bilateral low grade serous adenocarcinoma (ER/PR positive) at the age of 50. The maternal aunt (II: 5) also presented with ovarian cancer at age 50 (immunohistochemistry and mutation status is unknown). Given that the proband inherited the *BRCA1*:c.594_597del from her mother, the high incidence of breast and ovarian cancer in the family strongly implicates the truncating *BRCA1*:c.594_597del as a deleterious mutation. To further understand potential pathogenicity of each allele, loss of

heterozygosity (LOH) analysis was performed on genomic DNA extracted from the tumors of the proband and her mother (Fig. 2B). Ovarian cancer tumor blocks from the mother (II: 4) demonstrated loss of the wild-type *BRCA1* allele with retention of the *BRCA1*:c.594_597del allele, consistent with *BRCA1*:c.594_597del as a deleterious mutation. Interestingly, in the proband, who carries both *BRCA1*:c.594_597del and c.5095C>T alterations, the breast tumor did not display LOH at either *BRCA1* allele, suggesting both mutant genes were dysfunctional and therefore no selective pressure existed in the tumor to lose either allele.

To further investigate the extent of BRCA1 deficiency in the proband, we performed an immunoblot for BRCA1 on primary skin fibroblast lysates from the proband (KFB14-1 cells) and sibling III: 3 (KFB14-2 cells). KFB14-1 cells showed significantly reduced expression of full length BRCA1 (Fig. 3A) in comparison to KFB14-2 cells, in agreement with reported in vitro experiments documenting that p.Arg1699Trp leads to BRCT misfolding and reduced proteolytic stability (16). RT-PCR and sequencing of the cDNA from the KFB14-1 cells demonstrated that most of the carboxy-terminal expressed BRCA1 mRNA in the proband carried the p.Arg1699Trp mutation (Fig. 3B), consistent with a nonsense mediated decay process reducing levels of the *BRCA1*:c.594_597del mRNA. Given the known involvement of BRCA1 in ICL repair and the clinical similarities to FA, chromosomal breakage tests were performed on peripheral blood lymphocyte and proband skin fibroblast cultures. Upon treatment with diepoxybutane (DEB), proband lymphocytes showed increased chromosomal breakage and radial chromosome formation (30% of cells displayed radial chromosomes at 0.2 µg/mL DEB), which are well within the range established for a diagnosis of FA (Fig. 3C, 3D) (17). Mitomycin C (MMC) treated skin fibroblast cultures from the proband also exhibited increased radial chromosomes in comparison to heterozygous sibling control fibroblasts, although quantification was not possible due to a failure to obtain sufficient numbers of proband fibroblast metaphases (Fig. 3C). These cellular data, in concert with the clinical presentations of growth failure, microcephaly, dysmorphic faces and other congenital anomalies are supportive of a diagnosis of FA-like disorder in the proband.

BRCA1 functions in genome integrity maintenance in part through delivery of RAD51 to DSBs for homologous recombination. Consistent with impaired DSB repair function, BRCA1 and Rad51 foci were present in only 24.27 % and 26.02 % of KFB14-1 cells at 6 hours following 10 Gy IR compared to 57.14% and 65.13 % of KFB14-2 cells (Fig. 4A, B). We next treated fibroblast cultures with MMC to test the integrity of FA-BRCA pathway function in proband cells in ICL repair. Similar to the condition of IR, MMC treated KFB14-1 cells showed less BRCA1 and Rad51 foci (30.56 % and 28.89 % respectively) compared to KFB14-2 cells (66.26 % and 62.5 % respectively) (Fig. 3B, Supplementary Fig. S1). To further ascertain whether mutant BRCA1 exhibited deficiency in DSB recognition, we examined localization of an epitope tagged carboxy-terminal region of BRCA1 containing the BRCT repeats to nuclease induced breaks present within a single genomic location in U2OS cells (Supplementary Fig. S2). The BRCA1 fragment containing p.Arg1699Trp was observed at 22.11% of DSBs, similar to another known cancer related BRCT mutant p.Pro1749Arg (20.11% of DSBs, $p = 0.059$), but significantly less than the

wild-type (WT) BRCT fragment (73.58%, $p = 0.003$). Interestingly, the p.Val1736Ala mutation found in the other biallelic carrier yielded an intermediate deficit in DSB localization, consistent with her less severe clinical presentation of developmental anomalies (12) and the less direct interaction of Val1736 with BRCT binding phospho-proteins (Supplementary Fig. S2).

BRCA mutant and other HR-deficient cells are exquisitely sensitive to PARP (poly-ADP ribose polymerase 1 and 2) inhibition (18, 19). KFB14-1 cells were hypersensitive to the PARP inhibitor Olaparib (LC50: 2.66 μM) in comparison to KFB14-2 cells (LC50: 25.1 μM) (Fig. 4C). Moreover, Olaparib treatment for 36 h, revealed persistent γH2AX foci in proband derived KB14-1 cells in comparison to sibling control KFB14-2 cells (Supplementary Fig. S3). These results strongly suggest defective BRCA1 dependent DNA repair in KFB14-1 cells. To verify that the pathogenic phenotype is due to the deficiency of BRCA1, we complemented the KFB14-1 cells by retroviral transduction of a cDNA expressing BRCA1 with wildtype BRCT repeats. Due to the difficulty of stable reconstitution with full length BRCA1 in primary cells, we utilized a *BRCA1* 512-1283 transgene, which has been reported to restore radiation resistance in BRCA1- BRCT mutant breast cancer cells (20). When complemented with *BRCA1* 512-1283, KFB14-1 cells recovered Rad51 foci formation after IR or MMC exposure (Fig. 4A, B). Furthermore, *BRCA1* 512-1283 reconstitution restored resistance in KFB-1 cells to Olaparib and to MMC (Fig. 4C, D).

DISCUSSION

This study demonstrates that biallelic *BRCA1* mutations cause a FA-like cellular and clinical phenotype in a human patient. The only other known patient with biallelic *BRCA1* mutations also had a missense mutation in the BRCT repeats and presented similarly to the proband in this study with microcephaly, short stature and developmental delays. Although the chromosomal breakage test was not available, the other patient experienced significant toxicity from carboplatin, suggestive of hypersensitivity to interstrand crosslink reagents. In both cases, the patients had either breast or ovarian cancer, but did not develop bone marrow failure, which is similar to the FA-O (RAD51C) complementation group (21–23). It would appear prudent, however, to follow hematologic indices in patients with biallelic *BRCA1* mutations (FANCS) until more data are available.

The viability of biallelic *BRCA1* mutations also has important implications for genetic counseling. These two patients, together, indicate that there is a risk for couples in which each partner harbors a pathogenic *BRCA1* mutation of having a child with FA-S, particularly when one of the alleles is a missense change to the BRCT repeats. On a more general note, this study demonstrates the importance of looking at all genes in a WES study, and highlights the overlap between incidental and diagnostic findings.

Biallelic *BRCA2* and *PALB2* mutations cause a severe FA phenotype and a distinct tumor spectrum from breast and ovarian cancer, which predominate when mutations occur in the heterozygous state (9–11). Although only two patients with biallelic mutations in *BRCA1* have been reported, it is interesting to note that both maintained the breast and ovarian

cancer predilection of *BRCA1* carriers and neither displayed spontaneous bone marrow failure. This small sample size is suggestive of different phenotypic manifestations of biallelic *BRCA1* mutations in comparison to biallelic mutations in either *BRCA2* or *PALB2*. We posit that HR deficiency contributes to the observed phenotypes in the proband. This is based on our findings of reduced Rad51 foci formation and PARPi hypersensitivity in the proband's fibroblasts. In addition, the *BRCA1* BRCT repeats are important for early stages of ICL recognition (7). It is thus possible that multiple aspects of ICL repair function are compromised in FANCS patients and contribute to the observed phenotypes. We also acknowledge that it is possible that mutations outside of the *BRCA1* BRCT repeats could support viability in humans and lead to a different clinical presentation than either of the two reported *BRCA1* compound heterozygotes. Nonetheless, the combination of clinical and cellular findings reveals additional complexities in the phenotypic manifestations of biallelic mutations within proximal and distal arms of ICL repair. Moreover, they demonstrate that specific combinations of deleterious *BRCA1* (*FANCS*) mutations predispose to a new FA subtype with breast and ovarian cancer susceptibility.

METHODS

Samples and cell lines

The patient provided written informed consent in accordance with the Declaration of Helsinki before enrollment in this study and gave additional specific approval for the publication of full facial images. The Institutional Review Board and Ethical Committee approved this study. Skin fibroblast cells KFB14-1 and KFB14-2 were derived from proband III:2 and sibling III:3, respectively. Cells were maintained in DMEM: F12 mix (Invitrogen) with 10% fetal bovine serum and pen/strep. After 3–4 times passages, Sanger sequencing was used to confirm the originally assigned *BRCA1* gene sequences in the proband and sibling derived cell lines. U2OS-DSB-reporter cell line was cultured in DMEM (Invitrogen) with 10% calf serum and pen/strep. Stable expression of *BRCA1* 512-1283 fibroblast cell (KB14-1) was generated by retroviral transduction.

Antibodies and chemicals

Antibodies used for protein blots and immunofluorescence are as follows: mouse monoclonal anti-*BRCA1* antibody D9 (Santa Cruz Biotechnology); anti- γ H2AX (Millipore); anti-Rad51 (Santa Cruz Biotechnology); anti-RPA (Novus); anti-Cyclin A (Santa Cruz Biotechnology), Olaparib (ChemieTek), MMC (Sigma).

Whole Exome sequencing and data analysis

Patient DNA was extracted from whole blood using standard protocols. DNA samples were processed by the University of Washington Center for Mendelian Genomics (UW-CMG). The initial QC entails DNA quantification, sex typing, and molecular “fingerprinting” using a 96-plex genotyping assay. Library construction (using 1 μ g of genomic DNA) and exome capture are automated (Perkin-Elmer Janus II) in 96-well plate format. Libraries undergo exome capture using the ~37 Mb target from Roche/NimblegenSeqCap EZ v2.0. Prior to sequencing, library concentration is determined by triplicate qPCR and molecular weight distributions are verified on Agilent Bioanalyzer 2100. Individual exome multiplex-

compatible libraries are pooled into sets of 24–96 samples using liquid handling robotics. Sequencing-by-synthesis is carried out on the IlluminaHiSeq platform (2×50bp reads). Current throughput is sufficient to complete 3–4 multiplexed exomes per lane at high coverage (60–80x mean coverage).

Sequencing data processing involved: (1) base calling (Illumina RTA 1.13); (2) demultiplexing and conversion into unaligned BAM files by lane and index sequence (IlluminaBasecallsToSam and Picard ExtractIlluminaBarcodes); (3) alignment to the human reference (hg19/GRCh37) using BWA (24). Read-pairs not mapping within ± 2 standard deviations of the average library size ($\sim 125 \pm 15$ bp for exomes) were removed. Following QC, individual-level data was merged and subjected to the following steps: (1) base quality recalibration using GATK TableRecalibration; (2) reads with duplicate start positions were removed; (3) indel realignment using GATK IndelRealigner, and (4) variant calling using multiple samples with the UnifiedGenotyper routine of GATK 1.6–11 (25).

Variants observed in more than 10% of other UW-CMG samples prepared using the same capture probe set were removed and remaining variants filtered for $QUAL \geq 250$, $GQ \geq 30$, $QD \geq 5$, $Map35 \geq 0.99$, $AB \leq 0.8|NA$, absence of SnpCluster or HRunFilter flags, no InDels ± 5 bp, maximum 1000G/ESP frequency of 0.001 for denovo/dominant variants and 0.01 for recessive variants. Variants were annotated using Ensembl Variant Effect Predictor v2.6 (26) and the analysis limited to events with the following predicted consequences: FRAME_SHIFT, INFRAME, NONCODING_CHANGE, NON_SYNONYMOUS, CANONICAL_SPLICE, STOP_GAINED, STOP_LOST, UNKNOWN. In case of overlapping annotations or multiple isoforms, one annotation was picked based on whether the annotation was in CCDS, the availability and value of SIFT/PolyPhen scores, and the splice site distance.

Chromosome breakage studies

The lymphocyte cultures were established from whole blood as routinely applied to make chromosomal preparations for karyotype analysis. DEB was used at a final concentration of 0.1 – 0.22 $\mu\text{g/ml}$ for chromosome fragility tests in lymphocytes, and 0.1 $\mu\text{g/ml}$ in fibroblasts.

LOH analysis

Genomic DNA was extracted from paraffin-embedded tumor samples following laser capture microdissection (Skin Disease Research Center cores of University of Pennsylvania). Primers 5'-AGGAGAGAGCAGCTTTCAC-3', 5'-CTGATTTTCATCCCTGGTTCC-3' and 5'-CAGCCTCTGATTCTGTTCAC-3', 5'-TCCTCCCGCAATTCCTAG-3' were used to amplify Exon 10 and Exon 18 respectively. Sanger sequencing was performed on ABI3730 (University of Pennsylvania Genomics Facility).

Cell survival assay

Cell survival was assessed by Cell Titer 96® Aqueous Non-Radioactive Cell Proliferation Assay kits following manufacturer instruction (promega). Experiments were repeated three times, and data represented as the mean of six replicate wells \pm SEM.

Immunofluorescence

Cells grown on coverslips were fixed using 3% paraformaldehyde/2% sucrose solution. Fixed cells were permeabilized with 0.5% Triton X-100 in PBS for 5 min at 4°C. Following incubation with primary antibody for 20 mins at 37°C in humidified chamber, cells were washed with PBST and then incubated with secondary antibody for 20 mins at 37°C in humidified chamber. After extensive washing with PBST, coverslips were mounted onto glass slides using Vectashield mounting medium containing DAPI (Vector Laboratories).

Supplementary Material

Refer to Web version on PubMed Central for supplementary material.

ACKNOWLEDGEMENTS

The authors thank the patient and her family. Without their participation, this work would not have been possible. Sequencing was provided by the University of Washington Center for Mendelian Genomics (UW CMG) and was funded by the National Human Genome Research Institute and the National Heart, Lung and Blood Institute grant 1U54HG006493 to Drs. Debbie Nickerson, Jay Shendure and Michael Bamshad. The authors also thank A. D'Andrea (Dana-Farber Cancer Institute) for critical discussion of the data and the University of Pennsylvania Skin Disease Research Core for assistance with laser capture microdissection.

SUPPORT

This work was supported by NIH grants GM101149, CA138835, and CA17494, (to RAG) who is also supported by a DOD Breast Cancer Idea Award, a Harrington Discovery Institute Scholar-Innovator Award, and funds from the Abramson Family Cancer Research Institute and Basser Research Center for BRCA. DAD and KMB are supported by the CIHR Institute of Genetics Clinical Investigatorship Award. This patient was selected for study by the FORGE Canada Steering Committee, consisting of K. Boycott (U. Ottawa), J. Friedman (U. British Columbia), J. Michaud (U. Montreal), F. Bernier (U. Calgary), M. Brudno (U. Toronto), B. Fernandez (Memorial U.), B. Knoppers (McGill U.), M. Samuels (U. de Montreal) and S. Scherer (U. Toronto). This work was also funded in part by Genome Canada, the Canadian Institutes of Health Research (CIHR), the Ontario Genomics Institute (OGI-049), Genome Quebec and Genome British Columbia.

REFERENCES

1. Kottemann MC, Smogorzewska A. Fanconi anaemia and the repair of Watson and Crick DNA crosslinks. *Nature*. 2013; 493:356–363. [PubMed: 23325218]
2. D'Andrea AD, Grompe M. The Fanconi anaemia/BRCA pathway. *Nat Rev Cancer*. 2003; 3:23–34. [PubMed: 12509764]
3. Wang W. Emergence of a DNA-damage response network consisting of Fanconi anaemia and BRCA proteins. *Nat Rev Genet*. 2007; 8:735–748. [PubMed: 17768402]
4. Garaycochea JI, Patel KJ. Why does the bone marrow fail in Fanconi anemia? *Blood*. 2014; 123:26–34. [PubMed: 24200684]
5. Long DT, Raschle M, Joukov V, Walter JC. Mechanism of RAD51-dependent DNA interstrand cross-link repair. *Science*. 2011; 333:84–87. [PubMed: 21719678]
6. Raschle M, Knipscheer P, Enoiu M, Angelov T, Sun J, Griffith JD, et al. Mechanism of replication-coupled DNA interstrand crosslink repair. *Cell*. 2008; 134:969–980. [PubMed: 18805090]
7. Long DT, Joukov V, Budzowska M, Walter JC. BRCA1 Promotes Unloading of the CMG Helicase from a Stalled DNA Replication Fork. *Mol Cell*. 2014
8. Bunting SF, Callen E, Kozak ML, Kim JM, Wong N, Lopez-Contreras AJ, et al. BRCA1 Functions Independently of Homologous Recombination in DNA Interstrand Crosslink Repair. *Mol Cell*. 2012
9. Howlett NG, Taniguchi T, Olson S, Cox B, Waisfisz Q, De Die-Smulders C, et al. Biallelic inactivation of BRCA2 in Fanconi anemia. *Science*. 2002; 297:606–609. [PubMed: 12065746]

10. Xia B, Dorsman JC, Ameziane N, de Vries Y, Rooimans MA, Sheng Q, et al. Fanconi anemia is associated with a defect in the BRCA2 partner PALB2. *Nature Genet.* 2007; 39:159–161. [PubMed: 17200672]
11. Reid S, Schindler D, Hanenberg H, Barker K, Hanks S, Kalb R, et al. Biallelic mutations in PALB2 cause Fanconi anemia subtype FA-N and predispose to childhood cancer. *Nature Genet.* 2007; 39:162–164. [PubMed: 17200671]
12. Domchek SM, Tang J, Stopfer J, Lilli DR, Hamel N, Tischkowitz M, et al. Biallelic deleterious BRCA1 mutations in a woman with early-onset ovarian cancer. *Cancer Discov.* 2013; 3:399–405. [PubMed: 23269703]
13. Carvalho RS, Abreu RB, Velkova A, Marsillac S, Rodarte RS, Suarez-Kurtz G, et al. Probing structure-function relationships in missense variants in the carboxy-terminal region of BRCA1. *PLoS one.* 2014; 9:e97766. [PubMed: 24845084]
14. Spurdle AB, Whiley PJ, Thompson B, Feng B, Healey S, Brown MA, et al. BRCA1 R1699Q variant displaying ambiguous functional abrogation confers intermediate breast and ovarian cancer risk. *J Med Genet.* 2012; 49:525–532. [PubMed: 22889855]
15. Vallon-Christersson J, Cayan C, Haraldsson K, Loman N, Bergthorsson JT, Brondum-Nielsen K, et al. Functional analysis of BRCA1 C-terminal missense mutations identified in breast and ovarian cancer families. *Human Mol Genet.* 2001; 10:353–360. [PubMed: 11157798]
16. Coquelle N, Green R, Glover JN. Impact of BRCA1 BRCT domain missense substitutions on phosphopeptide recognition. *Biochemistry.* 2011; 50:4579–4589. [PubMed: 21473589]
17. Auerbach AD. Fanconi anemia and its diagnosis. *Mut Res.* 2009; 668:4–10. [PubMed: 19622403]
18. Bryant HE, Schultz N, Thomas HD, Parker KM, Flower D, Lopez E, et al. Specific killing of BRCA2-deficient tumours with inhibitors of poly(ADP-ribose) polymerase. *Nature.* 2005; 434:913–917. [PubMed: 15829966]
19. Farmer H, McCabe N, Lord CJ, Tutt AN, Johnson DA, Richardson TB, et al. Targeting the DNA repair defect in BRCA mutant cells as a therapeutic strategy. *Nature.* 2005; 434:917–921. [PubMed: 15829967]
20. Abbott DW, Thompson ME, Robinson-Benion C, Tomlinson G, Jensen RA, Holt JT. BRCA1 expression restores radiation resistance in BRCA1-defective cancer cells through enhancement of transcription-coupled DNA repair. *J Biol Chem.* 1999; 274:18808–18812. [PubMed: 10373498]
21. Vaz F, Hanenberg H, Schuster B, Barker K, Wiek C, Erven V, et al. Mutation of the RAD51C gene in a Fanconi anemia-like disorder. *Nature Genet.* 2010; 42:406–409. [PubMed: 20400963]
22. Meindl A, Hellebrand H, Wiek C, Erven V, Wappenschmidt B, Niederacher D, et al. Germline mutations in breast and ovarian cancer pedigrees establish RAD51C as a human cancer susceptibility gene. *Nature Genet.* 2010; 42:410–414. [PubMed: 20400964]
23. Loveday C, Turnbull C, Ruark E, Xicola RM, Ramsay E, Hughes D, et al. Germline RAD51C mutations confer susceptibility to ovarian cancer. *Nature Genet.* 2012; 44:475–476. [PubMed: 22538716]
24. Li H, Durbin R. Fast and accurate short read alignment with Burrows-Wheeler transform. *Bioinformatics.* 2009; 25:1754–1760. [PubMed: 19451168]
25. DePristo MA, Banks E, Poplin R, Garimella KV, Maguire JR, Hartl C, et al. A framework for variation discovery and genotyping using next-generation DNA sequencing data. *Nat Genet.* 2011; 43:491–498. [PubMed: 21478889]
26. McLaren W, Pritchard B, Rios D, Chen Y, Flicek P, Cunningham F. Deriving the consequences of genomic variants with the Ensembl API and SNP Effect Predictor. *Bioinformatics.* 2010; 26:2069–2070. [PubMed: 20562413]

SIGNIFICANCE

We establish that biallelic *BRCA1* mutations cause a distinct Fanconi Anemia subtype (FA-S), which has implications for risk counselling in families where both parents harbor *BRCA1* mutations. The genetic basis of hereditary cancer susceptibility syndromes provides diagnostic information, insights into treatment strategies, and more accurate recurrence risk counseling to families.

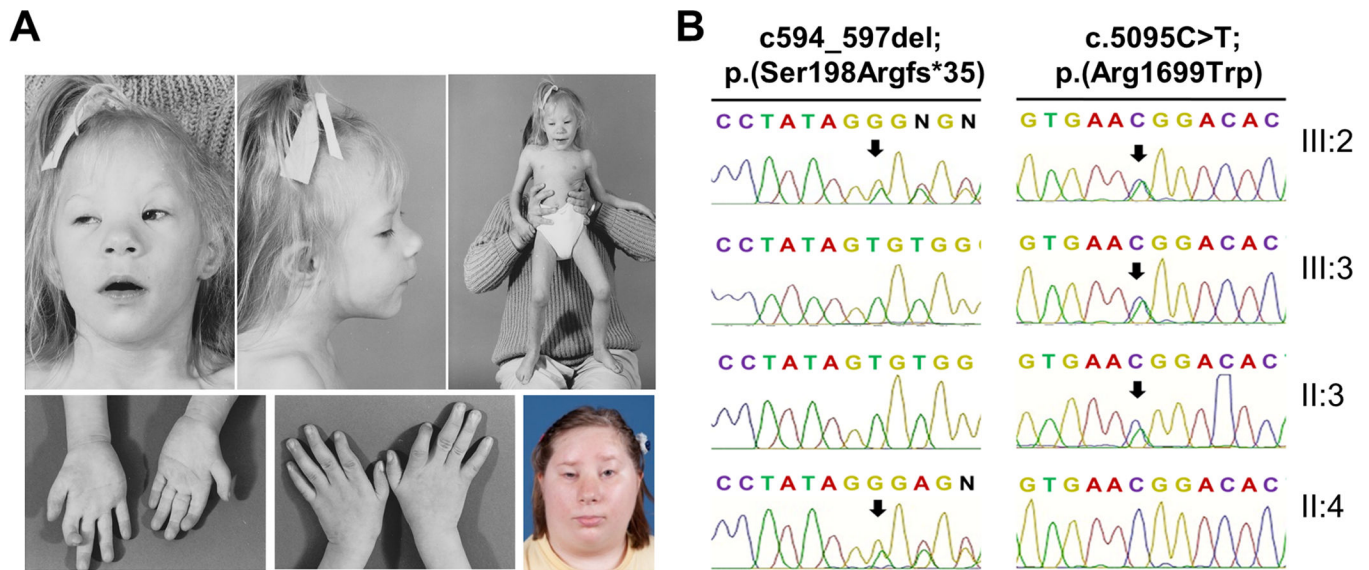
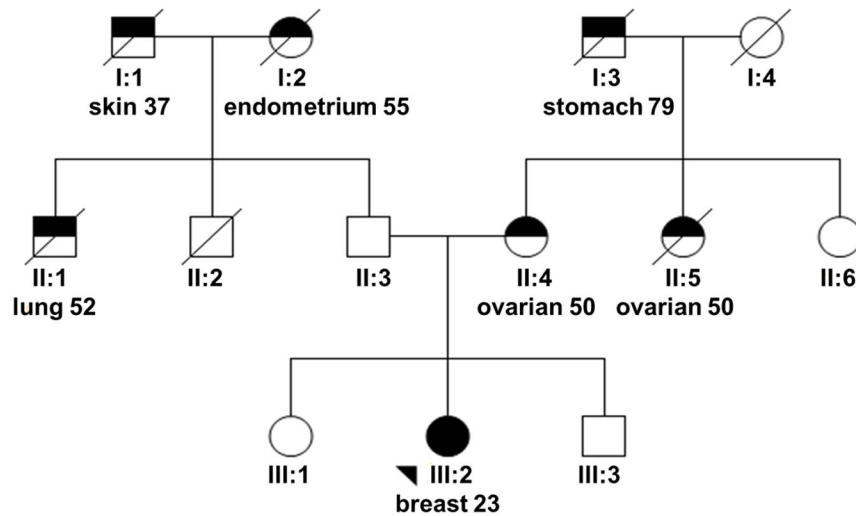
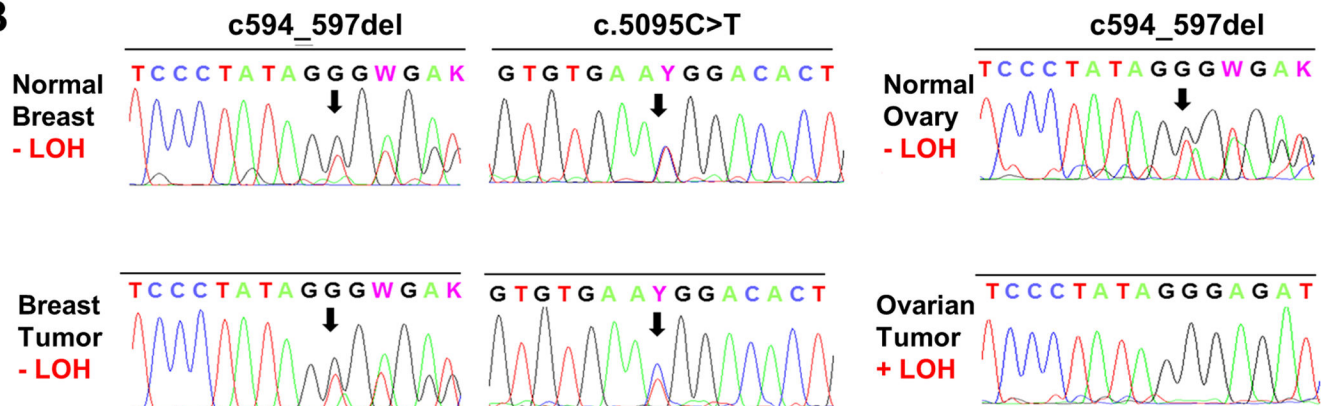


Figure 1.

An individual with early onset breast cancer, clinical features of Fanconi anemia, and biallelic *BRCA1* mutations. **A**, The affected individual at 3 and 23 years old showing hypertelorism, epicanthal folds, ptosis, strabismus, blepharophimosis, broad nasal bridge and nasal tip, and proximally inserted thumbs. **B**, Sequencing of *BRCA1* in family members demonstrated that both *BRCA1* alleles in the proband were inherited from the heterozygous parents. III: 2, proband; III: 3, brother; II: 3, father; II: 4, mother

A**B****Figure 2.**

Pedigree and LOH analysis of proband breast cancer. **A**, Pedigree with all known cancer diagnoses in the family. **B**, LOH analysis by Sanger sequencing of genomic DNA extracted from paraffin-embedded tumor blocks. Breast tumor was derived from the proband (III: 2), and ovarian cancer was derived from the mother (II: 4). Cancer cells and control non-cancer cells were isolated and enriched by laser capture microdissection (LCM).

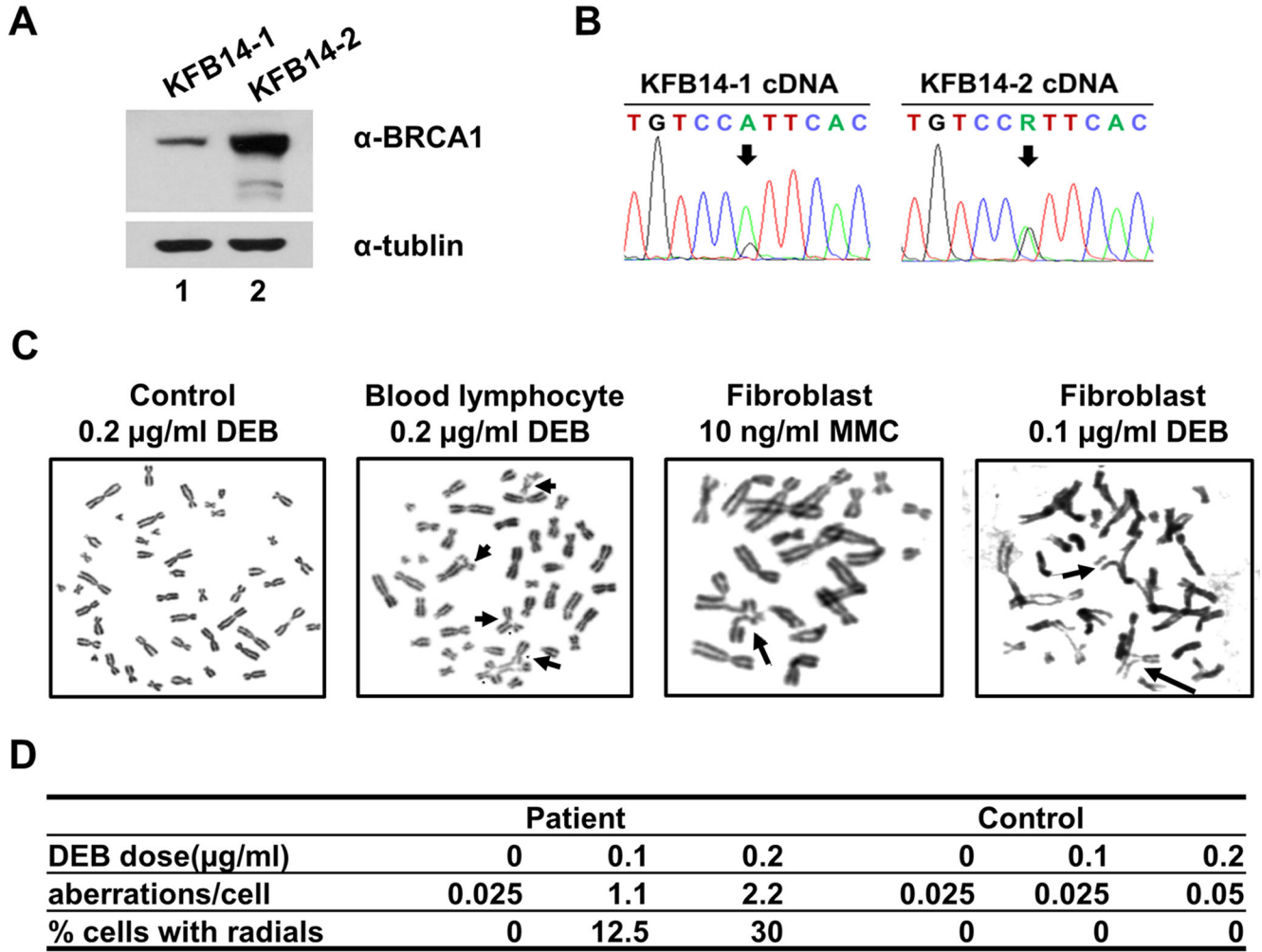
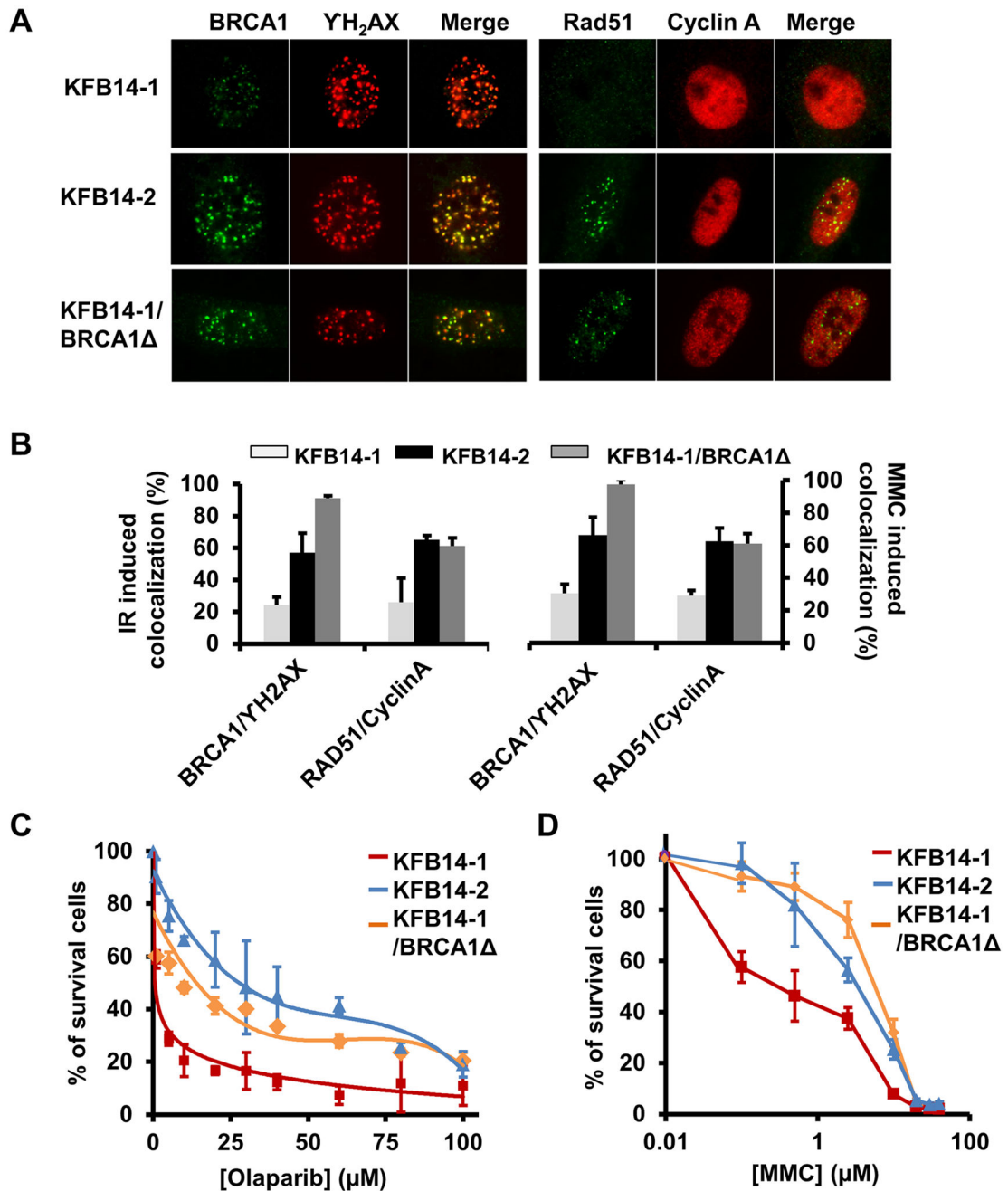


Figure 3.

Characterization of BRCA1 function in the proband derived cells. **A**, Immunoblot for BRCA1 from fibroblast cell lysates shows reduced BRCA1 expression in the proband compared to the heterozygous sibling. KFB14-1, fibroblast cells derived from the proband III: 2. KFB14-2, fibroblast cells derived from the sibling III: 3. **B**, RT-PCR followed by cDNA sequencing showed approximately 80% of *BRCA1* mRNA in KFB14-1 cells contains the p.Arg1699Trp mutation, while approximately 50% of *BRCA1* mRNA in KFB14-2 cells are wild type. **C**, Examples of metaphase chromosomes from peripheral blood lymphocytes (treated with 0.2 µg/ml diepoxybutane (DEB)) and fibroblast KFB14-1 cells (treated with 10ng/ml MMC or 0.1 µg/ml DEB). Arrows indicate radial chromosomes or chromatid breaks. **D**, Quantification of abnormal chromosomes in chromosome breakage tests from peripheral blood samples of the proband and sibling.

**Figure 4.**

Defective BRCA1 DNA repair function in proband derived cells. **A**, Immunofluorescence showing reduced BRCA1 and Rad51 foci formation at IR induced damage sites. Complementation of KFB14-1 cells with BRCA1 512-1283 (KFB14-1/BRCA1 Δ) restored BRCA1 and Rad51 foci formation. **B**, Quantification of the percentage of fibroblasts with BRCA1 and γ H2AX colocalization and/or percentage of Cyclin A positive cells with Rad51 foci. KFB14-1, KFB14-2 and KFB14-1/BRCA1 Δ cells were exposed to 10 (Gy) ionizing radiation or 0.5 μ M MMC for 24 hrs. Cells with ≥ 5 foci are scored as positive cells. **C,D**,

Cell survival (MTT) assay showing the survival curve of fibroblasts treated with PARP inhibitor Olaparib (C) or MMC (D). KFB14-1, KFB14-2 and KFB14-1/BRCA1 cells were treated with Olaparib or MMC at the indicated concentrations for 72 hrs. BRCA1 512-1283 successfully restored resistance to Olaparib or MMC in KFB14-1 cells. Error bars represent standard error of the mean from 3 independent experiments.